Atmos. Chem. Phys. Discuss., https://doi.org/10.5194/acp-2018-769
Manuscript under review for journal Atmos. Chem. Phys.
Discussion started: 3 September 2018

Atmospheric Chemistry and Physics Discussions

Aliphatic Carbonyl Compounds (C_8-C_{26}) in Wintertime Atmospheric Aerosol in London, UK

Ruihe Lyu[1,2], Mohammed Salim Alam[1], Christopher Stark[1]

Ruixin Xu[1], Zongbo Shi[2], Yinchang Feng[2] and Roy M. Harrison[†*1]

[1] Division of Environmental Health and Risk Management

School of Geography, Earth and Environmental Sciences, University of Birmingham Edgbaston, Birmingham B15 2TT, UK

[2] State Environmental Protection Key Laboratory of Urban Ambient Air Particulate Matter Pollution Prevention and Control, College of Environmental Science and Engineering

Nankai University, Tianjin 300350, China

† Also at: Department of Environmental Sciences / Centre of Excellence in Environmental Studies, King Abdulaziz University, PO Box 80203, Jeddah, 21589, Saudi Arabia.

Corresponding authors:
E-mail: r.m.harrison@bham.ac.uk (Roy M. Harrison)

Atmos. Chem. Phys. Discuss., https://doi.org/10.5194/acp-2018-769
Manuscript under review for journal Atmos. Chem. Phys.
Discussion started: 3 September 2018

Atmospheric Chemistry and Physics Discussions

ABSTRACT

Three groups of aliphatic carbonyl compounds, the n-alkanals (C8-C20), n-alkan-2-ones (C8-C26) and n-alkan-3-ones (C8-C19) were measured in air samples collected in London from January-April 2017. Four sites were sampled including two roof-top background sites, one ground-level urban background site and a street canyon location on Marylebone Road in central London. The n-alkanals showed the highest concentrations followed by the n-alkan-2-ones and the n-alkan-3-ones, the latter having appreciably lower concentrations. It seems likely that all compound groups have both primary and secondary sources and these are considered in the light of published laboratory work on the oxidation products of high molecular weight n-alkanes. All compound groups show relatively low correlation with black carbon and NOx in the background air of London, but in street canyon air heavily impacted by vehicle emissions, stronger correlations emerge especially for the n-alkanals. It appears that vehicle exhaust is likely to be a major contributor for concentrations of the n-alkanals whereas it is a much smaller contributor to the n-alkan-2-ones and n-alkan-3-ones. Other primary sources such as cooking may be significant but were not evaluated. It seems likely that there is also a significant contribution from photo-oxidation of n-alkanes and this would be consistent with the much higher abundance of the n-alkan-2-ones relative to the n-alkan-3-ones if the formation mechanism were to be through oxidation of condensed phase alkanes. Vapour-particle partitioning fitted the Pankow model well for the n-alkan-2-ones but less well for the other compound groups, although somewhat stronger relationships were seen at the Marylebone Road site than at the background sites.

Keywords: Carbonyl compounds; n-alkanals; n-alkan-2-ones; n-alkan-3-ones; organic aerosol; partitioning;

Atmos. Chem. Phys. Discuss., https://doi.org/10.5194/acp-2018-769
Manuscript under review for journal Atmos. Chem. Phys.
Discussion started: 3 September 2018

Atmospheric Chemistry and Physics Discussions

1. INTRODUCTION

Carbonyl compounds are classified as polar organic compounds, constituting a portion of the oxygenated organic compounds in atmospheric particulate matter (PM). Aliphatic carbonyl compounds are directly emitted into the atmosphere from primary biogenic and anthropogenic sources (Schauer et al., 2001, 2002a, b), as well as being secondary products of atmospheric oxidation of hydrocarbons (Chacon-Madrid et al., 2010; Zhang et al., 2015; Han et al., 2016).

The most abundant atmospheric carbonyls are methanal (formaldehyde) and ethanal (acetaldehyde), and many studies have described their emission sources and chemical formation in urban and rural samples (Duan et al., 2016). Long-chain aliphatic carbonyl compounds have been identified in PM and reported in few published papers (Gogou et al., 1996; Andreou and Rapsomanikis, 2009), and these compounds are considered to be formed from atmospheric oxidation processes affecting biogenic emissions of alkanes. Anthropogenic activity is also considered to be a significant contributor to the aliphatic carbonyls. Appreciable concentrations of aliphatic carbonyl compounds have been identified in emissions from road vehicles (Schauer et al., 1999), coal combustion (Oros and Simoneit, 2000), wood burning (Rogge et al., 1998) and cooking processes (Zhao et al., 2007b, a), spanning a wide range of molecular weights. Furthermore, chamber studies (Chacon-Madrid and Donahue, 2011; Algrim and Ziemann, 2016) have demonstrated that the aliphatic carbonyl compounds are very important precursors of secondary organic aerosol (SOA) when they react with OH radicals in the presence of NO_x.

70 The oxidation of n-alkanes by hydroxyl radical is considered to be an important source of carbonyl
71 compounds. It was believed that the n-alkanals with carbon atoms numbering less than 20 indicate
72 oxidation of alkanes, whereas the higher compounds were usually considered to be of direct biogenic
73 origin (Rogge et al., 1998). The homologues and isomers of n-alkanals and n-alkanones have been
74 identified as OH oxidation products of n-alkanes in many chamber and flow tube studies (Zhang et
75 al., 2015; Schilling Fahnestock et al., 2015; Ruehl et al., 2013). The commonly accepted oxidation
76 pathways of n-alkanes generally divide into functionalization and fragmentation. Functionalization
77 occurs when an oxygenated functional group (–ONO_2, –OH, –C=O, –C(O)O– and –OOH) is added
78 to a molecule, leaving the carbon skeleton intact. Alternatively, fragmentation involves C−C bond
79 cleavage and produces two oxidation products with smaller carbon numbers than the reactant. The
80 chamber studies of dodecane oxidation have identified 1-undecanal, hexan-3-one, octan-3-one,
81 heptan-2-one, nonan-2-one and decan-2-one as OH oxidation products (Schilling Fahnestock et al.,
82 2015; Yee et al., 2012).
83
84 In London, with a high population density and a large number of diesel engine vehicles, the aliphatic
85 hydrocarbons constitute an important fraction of ambient aerosols. Anthropogenic activities and
86 secondary formation favour the emission and production of carbonyl compounds within the city. The
87 objectives of the present study were the identification and quantification of aliphatic carbonyl
88 compounds in particle and vapour samples collected in London from January to April 2017. This
89 work has aided an understanding of the concentrations and secondary formation of carbonyls in the
90 London atmosphere. Spatial and temporal variations of the studied carbonyl compounds were
91 assessed and used to infer sources. One of the main objectives was to provide gas/particle partitioning

coefficients of identified carbonyls under realistic conditions. Diagnostic criteria were used to estimate the sources of identifiable atmospheric carbonyl compounds. Additionally, for the first time, concentrations of particulate and gaseous n-alkan-3-ones are reported.

2. MATERIALS AND METHODS

2.1 Sampling Method and Site Characteristics

Three sampling campaigns were carried out between 23 January and 18 April 2017 at four sampling sites (Figure 1) in London. The first campaign used two sampling sites, one located on the roof of a building (15 m above ground) of the Regent's University (51°31′N, -0°9′W), hereafter referred to as RU, sampled from 23 January 2017 to 19 February 2017, the other located on the roof (20 m above ground) of a building which belongs to the University of Westminster on the southern side of Marylebone Road (hereafter referred to as WM), sampled from 24 January 2017 to 20 February 2017. The third sampling site was located at ground level at Eltham (51°27′N, 0°4′E), hereafter referred to as EL, sampled from 23 February 2017 to 21 March 2017, which is located in suburban south London, and the fourth sampling site was located at ground level on the southern side of Marylebone Road (51°31′N, -0°9′W), hereafter referred to as MR, sampled from 22 March 2017 to 18 April 2017. Marylebone Road is in London's commercial centre, and is an important thoroughfare carrying 80-90,000 vehicles per day through central London. The Regent's University site is within Regent's Park to the north of Marylebone Road. The Eltham site is in a typical residential neighbourhood, 22 km from the MR site. Earlier work at the Marylebone Road and a separate Regent's Park site is described by Harrison et al. (2012).

The particle samples were collected on polypropylene backed PTFE filters (47 mm, Whatman) which preceded stainless steel sorbent tubes packed with 1cm quartz wool, 300 mg Carbograph 2TD 40/60 (Markes International, Llantrisant, UK) and sealed with stainless-steel caps before and after sampling. Sampling took place for sequential 24-hour periods at a flow rate of 1.5 L min^{-1} using an in-house developed automated sampler. Field blank filters and adsorption tubes were prepared for each site, and recovery efficiencies were evaluated. After the sampling, each filter was placed in a clean sealed petri dish, wrapped in aluminium foil and stored in the freezer at -18ºC prior to analysis. Black carbon (BC) was simultaneously monitored during the sampling period at RU and WM sites using an aethalometer (Model AE22, Magee Science). Measurements of BC and NO_x at MR and NO_x at EL were provided by the national network sites of Marylebone Road, and Eltham (https://uk-air.defra.gov.uk/).

2.2 Analytical Instrumentation

The particle samples were analyzed using a 2D gas chromatograph (GC, 7890A, Agilent Technologies, Wilmington, DE, USA) equipped with a Zoex ZX2 cryogenic modulator (Houston, TX, USA). The first dimension was equipped with a SGE DBX5, non-polar capillary column (30.0 m, 0.25 mm ID, 0.25 mm – 5.00% phenyl polysilphenylene-siloxane), and the second-dimension column equipped with a SGE DBX50 (4.00 m, 0.10 mm ID, 0.10 mm – 50.0% phenyl polysilphenylene-siloxane). The GC × GC was interfaced with a Bench-ToF-Select, time-of-flight mass spectrometer (ToF-MS, Markes International, Llantrisant, UK). The acquisition speed was 50.0 Hz with a mass resolution of >1200 fwhm at 70.0 eV and the mass range was 35.0 to 600 m/z. All data produced were processed using GC Image v2.5 (Zoex Corporation, Houston, US).

Atmos. Chem. Phys. Discuss., https://doi.org/10.5194/acp-2018-769
Manuscript under review for journal Atmos. Chem. Phys.
Discussion started: 3 September 2018

135 **2.3 Analysis of Samples**

136 Standards used in these experiments included 19 alkanes, C_8 to C_{26} (Sigma-Aldrich, UK, purity
137 >99.2%); 12 n-aldehydes, C_8 to C_{13} (Sigma-Aldrich, UK, purity ≥95.0%), C_{14} to C_{18} (Tokyo
138 Chemical Industry UK Ltd, purity >95.0%); and 10 2-ketones, C_8 to C_{13} and C_{15} to C_{18} (Sigma-
139 Aldrich, UK, purity ≥98.0%) and C_{14} (Tokyo Chemical Industry UK Ltd, purity 97.0%).

140

141 The filters were spiked with 30.0 µL of 30.0 µg mL^{-1} deuterated internal standards (dodecane-d_{26},
142 pentadecane-d_{32}, eicosane-d_{42}, pentacosane-d_{52}, triacontane-d_{62}, butylbenzene-d_{14}, nonylbenzene-
143 2,3,4,5,6-d_5, biphenyl-d_{10}, p-terphenyl-d_{14}; Sigma-Aldrich, UK) for quantification and then
144 immersed in dichloromethane (DCM), and ultra-sonicated for 20.0 min at 20.0ºC. The extract was
145 filtered using a clean glass pipette column packed with glass wool and anhydrous Na_2SO_4, and
146 concentrated to 50.0 µL under a gentle flow of nitrogen for analysis using GC × GC-ToF-MS. 1 µL
147 of the extracted sample was injected in a split ratio 100:1 at 300ºC. The initial temperature of the
148 primary oven (80.0ºC) was held for 2.0 min and then increased at 2.0 ºC min^{-1} to 210ºC, followed by
149 1.5 ºC min^{-1} to 325 ºC. The initial temperature of the secondary oven (120ºC) was held for 2.0 min
150 and then increased at 3.0ºC min^{-1} to 200ºC, followed by 2.00ºC min^{-1} to 300ºC and a final increase
151 of 1.0ºC min^{-1} to 330 ºC to ensure all species passed through the column. The transfer line
152 temperature was 330 ºC and the ion source temperature was 280ºC. Helium was used as the carrier
153 gas at a constant flow rate of 1.0 mL min^{-1}. Further details of the instrumentation and data processing
154 methods is given by Alam et al. (2016a,b).

155

156 The sorbent tubes were analyzed by an injection port thermal desorption unit (Unity 2, Markes
157 International, Llantrisant, UK) and subsequently analyzed using GC × GC-ToF-MS. Briefly, the
158 tubes were spiked with 1 ng of deuterated internal standard for quantification and desorbed onto the
159 cold trap at 350ºC for 15.0 min (trap held at 20.0ºC). The trap was then purged onto the column in
160 a split ratio of 100:1 at 350ºC and held for 4.0 min. The initial temperature of the primary oven
161 (90.0ºC) was held for 2.0 min and then increased to 2.0ºC min^{-1} to 240ºC, followed by 3.0ºC min^{-1}
162 to 310ºC and held for 5.0 min. The initial temperature of the secondary oven (40.0ºC) was held for
163 2.0 min and then increased at 3.0ºC min^{-1} to 250ºC, followed by an increase of 1.5ºC min^{-1} to 315ºC
164 and held for 5.0 min. Helium was used as carrier gas for the thermally desorbed organic compounds,
165 with a gas flow rate of 1.0 mL min^{-1}.

166

167 *Qualitative analysis*

168 Compound identification was based on the GC×GC-TOFMS spectra library, NIST mass spectral
169 library and in conjunction with authentic standards. Compounds within the homologous series for
170 which standards were not available were identified by comparing their retention time interval between
171 their homologues, and by comparison of mass spectra to the standards for similar compounds within
172 the series, by comparison to the NIST mass spectral library and by the analysis of fragmentation
173 patterns.

174

175 *Quantitative analysis*

176 An internal standard solution (including dodecane-d_{26}, pentadecane-d_{32}, eicosane-d_{42}, pentacosane-
177 d_{52}, triacontane-d_{62}, nonylbenzene-2,3,4,5,6-d_5, butylbenzene-d_{14}, biphenyl-d_{10}, p-terphenyl-d_{14})

(Sigma-Aldrich, UK) was added to the samples to extract prior to instrumental analysis. Five internal standards (pentadecane-d_{32}, eicosane-d_{42}, pentacosane-d_{52}, triacontane-d_{62}, nonylbenzene-2,3,4,5,6-d_5) were used in the calculation of carbonyl compound concentrations.

The quantification for alkanes, aldehydes and 2-ketones was performed by the linear regression method using seven-point calibration curves (0.05, 0.10, 0.25, 0.50, 1.00, 2.00, 3.00 ng μL^{-1}) established between the authentic standards/internal standard concentration ratios and the corresponding peak area ratios. The calibration curves for all target compounds were highly linear (r^2>0.99, from 0.990 to 0.997), demonstrating the consistency and reproducibility of this method. Limits of detection for individual compounds were typically in the range 0.04–0.12 ng m^{-3}. 3-ketones were quantified using the calibration curves for 2-ketones. This applicability of quantification of individual compounds using isomers of the same compound functionality (which have authentic standards) has been discussed elsewhere and has a reported uncertainty of 24% (Alam et al., 2018).

Alkan-2-ones and alkan-3-ones were not well separated by the chromatography. These were separated manually using the peak cutting tool, attributing fragments at m/z 58 and 71 to 2-ketones and m/z 72 and 85 to 3-ketones. The calibration for 2-ketones was applied to quantification of the 3-ketones.

Field and laboratory blanks were routinely analysed to evaluate analytical bias and precision. Blank levels of individual analytes were normally very low and in most cases not detectable. Recovery efficiencies were determined by analyzing the blank samples spiked with standard compounds. Mean

recoveries ranged between 78.0 and 102%. All quantities reported here have been corrected according to their recovery efficiencies.

3. RESULTS AND DISCUSSION

3.1 Mass Concentration of Particle-Bound Carbonyl Compounds

Fig. 2 shows the average total concentrations of particle-bound 1-alkanals, n-alkan-2-ones, and n-alkan-3-ones from January to April at four measurement sites, and the particle and gaseous phase concentrations are detailed in the Table S1 (Supporting Information). Total n-alkanals was defined as the sum of particle-bound n-alkanals ranging from C_8 to C_{20}. The particulate n-alkanals at the MR site accounted for 75.2% of the measured particle carbonyls with the average total concentration of 682 ng m^{-3}, and concentrations at the other sites were 167 ng m^{-3} at EL, 117 ng m^{-3} at WM and 82.6 ng m^{-3} at RU, accounting for 57.0%, 57.9% and 56.3% of the measured particulate carbonyls, respectively. The n-alkanals identified in this study differed in some aspects from those previously reported in samples collected from Crete (Gogou et al., 1996) and Athens (Andreou and Rapsomanikis, 2009) in Greece. The n-alkanals from London presented narrower ranges of carbon numbers and a higher concentration than rural and urban samples from Crete. The concentrations of n-alkanal homologues (C_8-C_{20}) ranged from 5.50 to 141 ng m^{-3} (average 52.0 ng m^{-3}) at MR which were far higher than 1.48-28.6 ng m^{-3} (average 6.44 ng m^{-3}) at RU, 1.42-50.3 ng m^{-3} (average 9.03 ng m^{-3}) at WM and 3.29-53.0 ng m^{-3} (average 13.0 ng m^{-3}) at EL (Table S1), unlike Crete where the concentrations were 0.9-3.7 ng m^{-3} in rural (C_{15}-C_{30}) and 5.4-6.7 ng m^{-3} in urban (C_9-C_{22}) samples, and the average concentration of all four sites was much higher than the 0.91 ng m^{-3} measured in Athens (Andreou and Rapsomanikis, 2009) (C_{13}-C_{20}).

As part of the CARBOSOL project (Oliveira et al., 2007), air samples were collected in summer and winter at six rural sites across Europe. The particulate n-alkanals ranged from C_{11} to C_{30} with average total concentrations between 1.0 ng m^{-3} and 19.0 ng m^{-3}, with higher concentrations in summer than winter at all but one site. These concentrations fall well below those measured in the present study, although the range of compounds differed. Maximum concentrations at all sites were in compounds >C_{22} indicating a source from leaf surface abrasion products and biomass burning. This far exceeds the C_{max} values seen in the particulate fraction at our sites.

The n-alkan-2-one homologues measured in London ranged from C_8 to C_{26}, and the average total particulate fraction concentration was 58.5 ng m^{-3} at RU, 75.1 ng m^{-3} at WM, 112 ng m^{-3} at EL and 186 ng m^{-3} at MR, approximately accounting for 39.9% (RU), 37.0% (WM), 38.1% (EL) and 20.5% (MR) of the total particulate carbonyls, respectively (Fig. 2). The published data from Greece indicated that the concentrations of n-alkan-2-ones were independent of the seasons, and an average of 5.40 ng m^{-3} (C_{13}-C_{29}) was measured in August and 5.44 ng m^{-3} in March at Athinas St, but 12.88 ng m^{-3} was measured in March at the elevated (20 m) AEDA site in Athens (Gogou et al. (1996). Concentrations in Crete for alkan-2-ones (C_{10}-C_{31}) were 0.4-2.1 ng m^{-3} at the rural site and 1.9-2.6 ng m^{-3} at the urban site (Andreou and Rapsomanikis, 2009).

The CARBOSOL project also determined concentrations of n-alkan-2-ones, between C_{14} and C_{31} with a C_{max} at C_{28} or C_{29} at all but one site. Average concentrations ranged from 0.15 ng m^{-3} (C_{17-29}) to 3.35 (C_{14}-C_{31}), very much below the concentrations at our London sampling site. Cheng et al. (2006) measured concentrations of n-alkan-2-ones in the Lower Fraser Valley, Canada, in $PM_{2.5}$.

Samples collected in a road tunnel showed the highest concentrations, total 1.8-12.6 ng m^{-3} for C_{10}-C_{31}, and were higher in daytime than nighttime. Concentrations at a forest site were 1.1-7.2 ng m^{-3} without a diurnal pattern. Values of C_{max} ranged from $C_{16\text{-}17}$ at the road tunnel to C_{27} (secondary maximum) at the forest site. Values of CPI averaged across sites from 1.00 to 1.34, giving little evidence for a substantial biogenic input from higher plant waxes.

Atmospheric concentrations of long-chain n-alkan-3-ones have not previously been reported in the literature. The n-alkan-2-one and n-alkan-3-one homologues with few carbon atoms are believed mainly to originate as the fragmental products of n-alkanes (Yee et al., 2012; Schilling Fahnestock et al., 2015), whereas the higher compounds are mainly generated from functional pathways (Zhang et al., 2015; Ruehl et al., 2013). The n-alkan-3-one homologues identified in the samples ranged from C_8 to C_{19}, and the average of individual compound concentrations was 0.52 ng m^{-3} at RU, 0.94 ng m^{-3} at WM, 1.37 ng m^{-3} at EL and 3.34 ng m^{-3} at MR. The concentrations of n-alkan-3-ones at the four sites were lower than the n-alkanals and n-alkan-2-ones, and MR had the highest average total mass concentrations 39.4 ng m^{-3}, followed by 14.3 ng m^{-3} at EL, 10.4 ng m^{-3} at WM and 5.65 ng m^{-3} at RU, respectively.

Recently published studies have found that the isomeric distribution of first-generation oxidation products of n-alkanes depends strongly upon whether the reaction occurs in the gas phase or at the particle surface (Kwok and Atkinson, 1995; Ruehl et al., 2013). The homogeneous gas-phase oxidation occurs fast, and H-abstraction by OH radicals occurs at all carbon sites. The fractions of the OH radical reaction by H atom abstraction from n-decane at the 1-, 2-, 3-, 4- and 5-positions are

3.10%, 20.7%, 25.4%, 25.4%, and 25.4%, respectively, and the products from homogeneous reaction were generally in accord with structure-reactivity relationship (SRR) predictions (Kwok and Atkinson, 1995; Aschmann et al., 2001). Reaction of particulate n-alkanes is dominated by heterogeneous reactions with OH, and the H-abstraction occurs preferentially at the 2-position of the carbon chain (Zhang et al., 2015; Ruehl et al., 2013). The n-alkanes diffuse from the inner particle to the surface, where the OH will quickly attack the H atom of 1 and 2 position carbons. The intermediate products at the 2-position are relatively more stable than at the 1-position, and the products are dominated by oxidation of the 2-position. The isomeric carbonyls formed via OH-initiated heterogeneous reactions of n-octacosane (C_{28}) exhibit a pronounced preference at the 2-position of the molecule chain[18]. The n-octacosan-2-ones have the highest relative yield (1.00), followed by n-octacosan-3-ones (0.50), while other isomeric carbonyl yields were lower than 0.20. The same results were found in the subsequent chamber studies of n-alkanes (Zhang et al., 2015) (C_{20}, C_{22}, C_{24}) but not C_{18}. The main reason was that OH oxidation of C_{18} was dominated by the homogeneous reaction as a large fraction of C_{18} evaporated into the gas phase.

During the field experiment, the 1-alkanal homologues were abundant in all samples, and this could be explained by a strong impact of anthropogenic activities. Thus, the n-alkanals are considered to arise mainly from primary emission sources. Furthermore, the particulate form of the n-alkane homologues (C_{14}-C_{36}) identified in the samples ranged from 50-100% in contrast to the low MW n-alkanes (C_{11}-C_{13}). The H-abstraction by OH radicals may therefore have been dominated by heterogeneous reactions generating the higher concentrations of n-alkan-2-ones than n-alkan-3-ones that were found in all samples. The ratio of n-alkan-2-ones/n-alkan-3-ones (C_{11}-C_{18}) with the same

carbon atom number ranged from 2.35-11.3 at four measurement sites. Surprisingly, although the n-alkane (C_{11}-C_{13}) oxidation was expected to be dominated by homogeneous reactions, the n-alkan-2-one/n-alkan-3-one ratios were still greater than 2.00. The probable reason was that the lower molecular weight n-alkan-2-ones were significantly impacted by primary emission sources. Another likely reason is that the n-alkan-2-one and n-alkan-3-one homologues with lower carbon atom numbers originated in part from the fragmental products of higher n-alkanes (Yee et al., 2012; Schilling Fahnestock et al., 2015).

The ratios of n-alkan-2-ones/n-alkanes, n-alkan-3-ones/n-alkanes (with same carbon numbers) were calculated and are reported in Table S2. The n-alkan-3-ones with carbon numbers higher than C_{20} were not identified in the samples, indicating that both the homogeneous and heterogeneous reactions of higher molecular weight n-alkanes were slow, the former probably due to the low vapour phase presence of n-alkanes. The ratios of n-alkan-3-ones/n-alkanes at four measurement sites gradually increased from $C_{11,}$ and then decreased from C_{17}, while higher ratios of n-alkan-2-ones/n-alkanes were observed in the range from C_{17} to C_{22}, probably indicating a shift from homogeneous reactions to heterogeneous reactions with the increase of carbon numbers. The low ratios of n-alkan-2-ones/n-alkanes with carbon numbers from C_{23} to C_{26} were attributed to the low diffusion rate from the inner particle to the surface with the increasing carbon number of n-alkanes, even though heterogeneous reactions were the dominant pathway.

Atmos. Chem. Phys. Discuss., https://doi.org/10.5194/acp-2018-769
Manuscript under review for journal Atmos. Chem. Phys.
Discussion started: 3 September 2018

3.2 Temporal and Spatial Variations

The study of temporal and spatial variations of air pollutants can provide valuable information about their sources and atmospheric processing. The time series of particle-bound n-alkanals, n-alkan-2-ones, and n-alkan-3-ones are plotted in Fig. 3. It is clear that the concentrations of n-alkanals varied substantially with date, and were always higher than n-alkanones at four sites. It is also clear from Figure 2 that concentrations were broadly similar at the background sites, RU, WM and EL, but are elevated, especially for the n-alkanals, at MR. This is strongly indicative of a road traffic source.

3.3 Sources of Carbonyl Compounds

3.3.1 Homologue distribution and carbon preference index (CPI)

Fig. 4 shows the average concentrations, and molecular distributions of particle-bound carbonyl compounds at the four sites. The values of carbon preference index (CPI) were calculated to estimate the origin of carbonyl compounds, according to Bray and Evans (1961):

$$\mathrm{CPI} = \frac{1}{2}\left(\frac{\sum_4^m C_{2i+1}}{\sum_4^m C_{2i}} + \frac{\sum_4^m C_{2i+1}}{\sum_5^{m+1} C_{2i}}\right)$$

For n-alkanals and n-alkan-3-ones (m=9): $\mathrm{CPI} = \frac{1}{2}\left(\frac{\sum odd(C_9-C_{19})}{\sum even(C_8-C_{18})} + \frac{\sum odd(C_9-C_{19})}{\sum even(C_{10}-C_{20})}\right)$

For n-alkan-2-ones (m=12): $\mathrm{CPI} = \frac{1}{2}\left(\frac{\sum odd(C_9-C_{25})}{\sum even(C_8-C_{24})} + \frac{\sum odd(C_9-C_{25})}{\sum even(C_{10}-C_{26})}\right)$

where *i* takes values between 4 and *m*, and 5 and *m* as in the equation, and

m = 9 for n-alkanal and n-alkan-3-ones

m = 12 for n-alkan-2-ones

330 The carbon maximum number (C_{max}) was used to evaluate the relative contribution of the source and
331 exhibit the homologue distribution of highest concentration. Table. 1 presents the CPI and C_{max} of
332 particle-bound carbonyl compounds calculated in the current and other studies.

333 According to the low CPI (0.41-1.07) at four sites, the n-alkanal homologues with carbon number
334 from C_8 to C_{20} mainly originate from anthropogenic emissions or OH oxidation of anthropogenic
335 hydrocarbons. The particle-bound n-alkanals exhibited a similar distribution of carbon number from
336 January to April at four sites, and they had the same C_{max} at C_8 with concentration 28.6 ng m^{-3} at
337 RU, 50.3 ng m^{-3} at WM, 53.0 ng m^{-3} at EL and 141 ng m^{-3} at MR, respectively. This compound may
338 be a fragmentation product, oxidation product or primary emission. In addition, the distribution of
339 n-alkanals had a second concentration peak at C_{15} (MR) and C_{18} (RU, WM, and EL). The C_{18}
340 compound was observed accounting for the highest percentage of the total mass of n-alkanals in
341 some rural aerosol samples (Gogou et al., 1996) in Crete. Andreou and Rapsomanikis reported the
342 C_{max} as C_{15} or C_{17} in Athens (Andreou and Rapsomanikis, 2009) and attributed this to the oxidation
343 of n-alkanes. However, a C_{max} at C_{26} or C_{28} in urban Crete (Gogou et al., 1996) was observed,
344 suggestive of biogenic input. The homologue distribution and CPI of n-alkanals in this study differed
345 from those previous reports, and demonstrated weak biogenic input and a strong impact of
346 anthropogenic activities in the London samples.

347

348 In this study, n-alkan-2-ones have similar homologue distributions and C_{max} (C_{19} or C_{20}) (Table 2)
349 at RU, WM and EL sites, and the total concentration from C_{16} to C_{23} accounts for 76.0%, 76.1% and
350 68.0% of ∑n-alkan-2-ones, respectively. The CPI values for n-alkan-2-ones ranged from 0.57 to
351 1.23 at the RU, MR and WM sites and were not indicative of biogenic input, and were considered

to mainly originate from anthropogenic activities and OH oxidation of anthropogenic n-alkanes. At EL, the CPI of 1.57 is probably indicative of a biogenic contribution in suburban south London. A difference was observed at the MR site, the n-alkan-2-ones with carbon atoms numbering from C_{12} to C_{18} accounting for 72.0% of ∑n-alkan-2-ones, with the C_{max} being at C_{16}. The C_{max} of n-alkan-3-ones was at C_{16} at the MR site, at EL, C_{max} = C_{16}, WM, C_{max} = C_{17} and at RU, C_{max} = C_{17}, respectively.

3.3.2 The ratios of n-alkanes/n-alkanals

Diesel engine emission studies have been conducted previously in our group; details of the engine set up and exhaust sampling system are given elsewhere (Alam et al., 2016b). Briefly, the steady-state diesel engine operating conditions were at a load of 5.90 bar mean effective pressure (BMEP) and a speed of 1800 revolutions per minute (RPM), and samples (n=14) were collected both before a diesel oxidation catalyst (DOC) and after a diesel particulate filter (DPF). The n-alkanes (C_{12} - C_{37}) and 1-alkanals (C_9 - C_{18}) were quantified in the particle samples, while n-alkanones were not identified because their concentrations were lower than the limits of (detection 0.01–0.15 ng m^{-3}). The emission concentrations of n-alkanals ranged from 7.10 to 53.2 µg m^{-3} (before DOC) and 1.20 to 11.5 µg m^{-3} (after DPF), respectively, and the ratios of alkanes/alkanals (C_{12}-C_{18}) with the same carbon atom numbers ranged from 0.15 to 0.23 (before DOC) and 0.52 to 7.60 (after DPF). The n-alkane/n-alkanal (C_{12}-C_{18}) ratio at MR ranged from 0.92 to 5.03, while average ratios of 27.6 (RU), 22.1 (WM) and 15.1 (EL) were obtained, respectively. The similarity of the n-alkanes/n-alkanal ratio between MR and the engine studies (after DPF) strongly suggests that diesel vehicle emissions were the main source of 1-alkanals at MR.

374 The emission factors of total alkanes from diesel engines are reported to be 7 times greater than
375 gasoline engines (Perrone et al., 2014), with n-alkanals with carbon atoms numbering lower than C_{11}
376 being quantified in the exhaust from gasoline engines (Schauer et al., 2002b; Gentner et al., 2013).
377 The n-alkane/n-alkanal (C_8-C_{10}) ratio with the same carbon numbers ranged from 5.60 to 14.3,
378 suggesting that gasoline combustion may be another source of atmospheric n-alkanals.
379
380 Studies of n-alkanals showed that aldehydes have high reactivity when the OH radical attacks the
381 aldehyde moiety (Chacon-Madrid and Donahue, 2011; Chacon-Madrid et al., 2010), and the rate
382 constants are more than 3 times those of n-alkanes with the same carbon number. The mechanism
383 and rate constants of H-abstraction by OH detailed in the Master Chemical Mechanism (MCM,
384 v3.3.1), were obtained via http://mcm.leeds.ac.uk/MCM, and used in the evaluation of our data.
385

386 **3.3.3 Correlation analysis**

387 Insights into the sources of carbonyls can be gained from correlation analysis with black carbon (BC)
388 and NO_x. This has the advantage of comparing relative concentrations of pollutants, rather than
389 absolute concentrations. The latter are strongly affected by weather conditions, making inter-site
390 comparisons difficult when sampling did not occur simultaneously. In London, both black carbon
391 and NO_x arise very substantially from diesel vehicle emissions (Liu et al., 2014; Harrison et al.,
392 2012; Harrison and Beddows, 2017), and hence these are good measures of road traffic activity. The
393 concentrations of BC were simultaneously determined by the online instruments during the sampling
394 periods, with the average concentrations of 1.34, 1.94 and 3.58 μg m^{-3} at the RU, WM and MR sites,
395 respectively. The data for NO_x were provided by the national network sites, with the average

concentrations of 23.4 and 202 μg m^{-3} at the EL and MR sites, respectively. At the MR site, the concentrations of BC and NO_x averaged 5.00 μg m^{-3} and 281 μg m^{-3} when southerly winds were dominant compared to 2.60 and 128 μg m^{-3} for northerly winds. All correlations were carried out with the sum of particle and vapour phases for the carbonyl compounds, and strong (r^2 = 0.87) and weak (r^2 = 0.12) correlations between BC and NO_x were obtained when the southerly and northerly winds were prevalent at MR, respectively. Marylebone Road is a street canyon site where a vortex circulation is established by the wind. The effect is that on northerly wind sectors the sampling site on the southern side of the road samples near-background air, while on southerly wind sectors, the traffic pollution is carried to the sampling site, leading to elevated pollution levels affected heavily by the traffic emissions. The strong correlation between BC and NO_x with southerly wind sectors is a reflection of their emission from road traffic. In addition, the correlations between n-alkanals (C_8-C_{20}) and BC, and between n-alkanals (C_8-C_{20}) and NO_x were calculated to assess the contribution of vehicular emission (Table S3). The results showed that the correlations (r^2) between n-alkanals and BC gradually decreased from 0.61 (C_9) to 0.34 (C_{20}) at MR when the southerly winds were prevalent, indicating that the distribution of n-alkanals, and especially the lower MW compounds, was significantly impacted by the vehicular exhaust emissions. The average correlations at MR (southerly winds) between n-alkanals and BC, and between n-alkanals and NO_x were r^2 = 0.47 and r^2 = 0.32, respectively. These moderate correlations demonstrated that the vehicular emissions were a substantial source of n-alkanals at MR, and result in the high background concentrations of n-alkanals in London. The other probable sources of n-alkanals include cooking emissions, wood burning, photooxidation of hydrocarbons and industrial emissions. Poorer correlations between n-alkanals and BC (average r^2 = 0.15), and between n-alkanals and NO_x (average r^2 = 0.15) were

observed at MR in the north London background air sampled when northerly winds were prevalent. There were very weak correlations (average $r^2 < 0.10$) between n-alkanals and BC, and between n-alkanals and NO_x at the RU, WM and EL sites, which may be attributable to the high chemical reactivity of n-alkanals. High concentrations of furanones (γ-lactones) are generated via the photo-oxidation reaction of n-alkanals (Alves et al., 2001), and the total concentrations (particle and gas) were up to 376, 279, 347 and 318 ng m^{-3} at RU, WM, WL, and MR, respectively for the sum of furanone homologues (from 5-propyldihydro-2(3H)-furanone to 5-tetradecyldihydro-2(3H)-furanone).

The relationships (r^2 values) between BC and NO_x and the n-alkan-2-ones were low at all sites, but notably higher with southerly winds at MR (average $r^2 = 0.33$ and 0.35 for BC and NO_x respectively) than for northerly winds ($r^2 = 0.16$ and 0.03 respectively). This is strongly suggestive of a contribution from vehicle exhaust to n-alkan-2-one concentrations, but smaller than that for n-alkanals. In the case of the n-alkan-3-ones, correlations averaged $r^2 = 0.25$ with BC and $r^2 = 0.21$ for NO_x in southerly winds, compared to $r^2 = 0.08$ and $r^2 = 0.05$ respectively for northerly winds. This is also suggestive of a small, but not negligible contribution of vehicle emissions to n-alkan-3-ones. The very low correlations observed in background air for both n-alkan-2-ones and n-alkan-3-ones with BC and NO_x are suggestive of the importance of non-traffic sources, probably including oxidation of n-alkanes. The considerable predominance for n-alkan-2-one over n-alkan-3-one concentrations may be indicative of a formation pathway from oxidation of condensed phase n-alkanes, but this is speculative as primary emissions may be dominant.

Atmos. Chem. Phys. Discuss., https://doi.org/10.5194/acp-2018-769
Manuscript under review for journal Atmos. Chem. Phys.
Discussion started: 3 September 2018

3.4 The Partition Between Particle and Gas Phase

The partitioning coefficient K_p between particles and vapour was calculated in this study according to the following equation defined by Pankow (1994):

$$K_p = \frac{C_p}{C_g * TSP}$$

Where, C_p and C_g (μg m^{-3}) are the concentration of the compounds in the particulate phase and gaseous phase, respectively. TSP is the concentration of total suspended particulate matter (μg m^{-3}), which was estimated from the PM_{10} concentration (PM_{10}/TSP = 0.80), and daily average PM_{10} concentrations were taken from the national network sites. The partitioning coefficients K_p calculated from our data and the percentages in the particulate form are presented in Table 2. For the three types of carbonyls, the n-alkanals >C_{16}, n-alkan-2-ones >C_{19}, and n-alkan-3-ones > C_{18} were assumed to have negligible vapour concentrations, and the partitioning into the particulate phase gradually increased from C_8 to high molecular weight compounds.

Log Kp was regressed against vapour pressure (VP_T) for the relevant temperature derived from UManSysProp (http://umansysprop.seaes.manchester.ac.uk/) according to the following equation:

$$\text{Log } K_p = \text{m log}(VP_T) + b$$

The calculated log K_p versus log (VP_T) for the three types of carbonyls was calculated for each day, and the results appear in the Table S4. Data from four sites were over the temperature range 0.40–15.3 °C. A good fit to the data for n-alkan-2-ones (r^2 = 0.54–0.94 at RU, 0.64-0.93 at WM, 0.43-

463 0.95 EL and 0.45-0.89 at MR) was obtained. It is notable that the fit to the regression equation as
464 indicated by the r^2 value is appreciably higher at the MR site than at the other sites, especially in the
465 case of the alkan-3-ones. This is not easily explained, except perhaps by an increased particle surface
466 area at the MR site which may enhance the kinetics of gas-particle exchange, leading to partitioning
467 which is closer to equilibrium.

468

469 **4. CONCLUSIONS**

470 Three groups of carbonyl compounds were determined in the particle and gaseous phase in London
471 and concentrations are reported for n-alkanals (C_8-C_{20}), n-alkan-2-ones (C_8-C_{26}) and n-alkan-3-ones
472 (C_8-C_{19}). The Marylebone Road site has the highest concentration of particle-bound n-alkanals, and
473 the average total concentration was up to 682 ng m^{-3}, followed by 167 ng m^{-3} at EL, 117 ng m^{-3} at
474 WM and 82.6 ng m^{-3} at RU. The particulate n-alkanals were abundant in all samples at all four
475 measurement sites, accounting for more than 56.3% of total particle carbonyls. In addition, the
476 average total particle concentrations of n-alkan-2-ones and n-alkan-3-ones at four measurement sites
477 were in the range of 58.5-186 ng m^{-3} and 5.65-39.4 ng m^{-3}, respectively. Diagnostic criteria,
478 including molecular distribution, CPI, C_{max}, ratios and correlations, were used to assess the sources
479 and their contributions to carbonyl compounds. The three groups of carbonyls have similar
480 molecular distributions and C_{max} values at the four measurement sites, and their low CPI values
481 (0.41-1.57) at the four sites indicate a weak biogenic input during sampling campaigns. Heavily
482 traffic-influenced air and urban background air were measured at the MR site when southerly and
483 northerly winds were prevalent respectively; correlations of r^2 = 0.47 and r^2=0.32 were obtained
484 between n-alkanals and BC, and between between n-alkanals and NO_x, respectively in southerly

485 winds. Vehicle emissions appear to be an important source of n-alkanals, which is confirmed by the
486 similar ratios of n-alkanes/n-alkanals measured at MR (0.92-5.03) and in diesel engine exhaust
487 studies (0.52-7.6), resulting in a high background concentration in London. In addition, the OH-
488 initiated heterogeneous reactions of n-alkanes appear to be important sources of n-alkanones, even
489 though weak contributions from vehicular exhaust emissions were suggested by correlation analysis
490 with BC and NO_x in southerly winds at MR. Anthropogenic primary sources appear to account for
491 a large proportion of the alkan-2-one and alkan-3-one concentrations measured in London.
492
493 In addition, the partitioning coefficients of carbonyls were determined from the relative proportions
494 of the particle and gaseous phases of individual compounds. The results of field measurements of
495 partitioning between particle and vapour phases showed generally a better fit at MR than at the other
496 three sites. The n-alkan-2-ones have a better fit at four sites than the n-alkanals and n-alkan-3-ones,
497 with r^2 = 0.78 (0.54–0.94) at RU, 0.85 (0.64-0.93) at WM, 0.74 (0.43-0.95) EL and 0.70 (0.45-0.89)
498 at MR, respectively in a regression of log K_p versus the compound vapour pressure.
499

500 **ACKNOWLEDGEMENTS**

501 Primary collection of samples took place during the FASTER project which was funded by the
502 European Research Council (ERC-2012-AdG, Proposal No. 320821). The authors would also like
503 to thank the China Scholarship Council (CSC) for support to R.L., and the Natural Environment
504 Research Council for support under the Air Pollution and Human Health (APHH) programme
505 (NE/N007190/1).

REFERENCE

Alam, M. S., Stark, C., and Harrison, R. M.: Using variable ionization energy time-of-flight mass spectrometry with comprehensive GC×GC to identify isomeric species, Anal. Chem., 88, 4211-4220, http://www.doi.org/10.1021/acs.analchem.5b03122, 2016a.

Alam, M. S., Zeraati-Rezaei, S., Stark, C. P., Liang, Z., Xu, H., and Harrison, R. M.: The characterisation of diesel exhaust particles - composition, size distribution and partitioning, Faraday. Discuss., 189, 69-84, http://www.doi.org/10.1039/C5FD00185D, 2016b.

Alam, M. S., Zeraati-Rezaei, S., Liang, Z., Stark, C., Xu, H., MacKenzie, A. R., and Harrison, R. M.: Mapping and quantifying isomer sets of hydrocarbons (≥ C 12) in diesel exhaust, lubricating oil and diesel fuel samples using GC× GC-ToF-MS, Atmos. Meas. Tech., 11, 3047, https://doi.org/10.5194/amt-11-3047-2018, 2018.

Algrim, L. B., and Ziemann, P. J.: Effect of the Keto Group on yields and composition of organic aerosol formed from OH radical-initiated reactions of ketones in the presence of NO_x, J. Phys. Chem. A., 120, 6978-6989, http://www.doi.org/10.1021/acs.jpca.6b05839, 2016.

Alves, C., Pio, C., and Duarte, A.: Composition of extractable organic matter of air particles from rural and urban Portuguese areas, Atmos. Environ., 35, 5485-5496, https://doi.org/10.1016/S1352-2310(01)00243-6, 2001.

Andreou, G., and Rapsomanikis, S.: Origins of n-alkanes, carbonyl compounds and molecular biomarkers in atmospheric fine and coarse particles of Athens, Greece, Sci. Total. Environ., 407, 5750-5760, http://dx.doi.org/10.1016/j.scitotenv.2009.07.019, 2009.

Aschmann, S. M., Arey, J., and Atkinson, R.: Atmospheric chemistry of three C10 alkanes, J. Phys. Chem. A., 105, 7598-7606, http://www.doi.org/10.1021/jp010909j, 2001.

Bray, E., and Evans, E.: Distribution of n-paraffins as a clue to recognition of source beds, Geochim. Cosmochim. Ac., 22, 2-15, https://doi.org/10.1016/0016-7037(61)90069-2, 1961.

Chacon-Madrid, H., and Donahue, N.: Fragmentation vs. functionalization: chemical aging and organic aerosol formation, Atmos. Chem. Phys., 11, 10553-10563, https://doi.org/10.5194/acp-11-10553-2011, 2011.

Chacon-Madrid, H. J., Presto, A. A., and Donahue, N. M.: Functionalization vs. fragmentation: n-aldehyde oxidation mechanisms and secondary organic aerosol formation, Phys. Chem. Chem. Phys., 12, 13975-13982, http://www.doi.org/10.1039/C0CP00200C, 2010.

Cheng, Y., Li, S.-M., Leithead, A., and Brook, J. R.: Spatial and diurnal distributions of n-alkanes and n-alkan-2-ones on PM 2.5 aerosols in the Lower Fraser Valley, Canada, Atmos. Environ., 40, 2706-2720, https://doi.org/10.1016/j.atmosenv.2005.11.066, 2006.

550 Duan, H., Liu, X., Yan, M., Wu, Y., and Liu, Z.: Characteristics of carbonyls and volatile organic
551 compounds (VOCs) in residences in Beijing, China, Front. Env. Sci. Eng., 10, 73-84,
552 http://www.doi.org/10.1007/s11783-014-0743-0, 2016.
553
554 Gentner, D. R., Worton, D. R., Isaacman, G., Davis, L. C., Dallmann, T. R., Wood, E. C., Herndon,
555 S. C., Goldstein, A. H., and Harley, R. A.: Chemical composition of gas-phase organic carbon
556 emissions from motor vehicles and implications for ozone production, Environ. Sci. technol., 47,
557 11837-11848, http://www.doi.org/10.1021/es401470e, 2013.
558
559 Gogou, A., Stratigakis, N., Kanakidou, M., and Stephanou, E. G.: Organic aerosols in Eastern
560 Mediterranean: components source reconciliation by using molecular markers and atmospheric back
561 trajectories, Org. Geochem., 25, 79-96, https://doi.org/10.1016/S0146-6380(96)00105-2, 1996.
562
563 Han, Y., Kawamura, K., Chen, Q., and Mochida, M.: Formation of high-molecular-weight
564 compounds via the heterogeneous reactions of gaseous C8–C10 n-aldehydes in the presence of
565 atmospheric aerosol components, Atmos. Environ., 126, 290-297,
566 http://dx.doi.org/10.1016/j.atmosenv.2015.11.050, 2016.
567
568 Harrison, R., Dall'Osto, M., Beddows, D., Thorpe, A., Bloss, W., Allan, J., Coe, H., Dorsey, J.,
569 Gallagher, M., and Martin, C.: Atmospheric chemistry and physics in the atmosphere of a
570 developed megacity (London): an overview of the REPARTEE experiment and its conclusions,
571 Atmos. Chem. Phys., 12, 3065-3114, https://doi.org/10.5194/acp-12-3065-2012, 2012.
572
573 Harrison, R. M., and Beddows, D. C.: Efficacy of recent emissions controls on road vehicles in
574 Europe and implications for public health, Sci. Rep-UK., 7, 1152,
575 http://www.doi.org/10.1038/s41598-017-01135-2., 2017.
576
577 Kwok, E. S., and Atkinson, R.: Estimation of hydroxyl radical reaction rate constants for gas-phase
578 organic compounds using a structure-reactivity relationship: an update, Atmos. Environ., 29, 1685-
579 1695, https://doi.org/10.1016/1352-2310(95)00069-B, 1995.
580
581 Liu, D., Allan, J., Young, D., Coe, H., Beddows, D., Fleming, Z., Flynn, M., Gallagher, M.,
582 Harrison, R., and Lee, J.: Size distribution, mixing state and source apportionments of black carbon
583 aerosols in London during winter time, Atmos. Chem. Phys., 14, https://doi.org/10.5194/acp-14-
584 10061-2014, 2014.
585
586 Oliveira, T. S., Pio, C., Alves, C. A., Silvestre, A. J., Evtyugina, M., Afonso, J., Fialho, P., Legrand,
587 M., Puxbaum, H., and Gelencsér, A.: Seasonal variation of particulate lipophilic organic
588 compounds at nonurban sites in Europe, J. Geophys. Res-Atmos., 112,
589 https://doi.org/10.1029/2007JD008504 2007.
590
591 Oros, D. R., and Simoneit, B. R. T.: Identification and emission rates of molecular tracers in coal
592 smoke particulate matter, Fuel., 79, 515-536, http://dx.doi.org/10.1016/S0016-2361(99)00153-2,
593 2000.

Pankow, J. F.: An absorption model of gas/particle partitioning of organic compounds in the atmosphere, Atmos. Environ., 28, 185-188, https://doi.org/10.1016/1352-2310(94)90093-0, 1994.

Perrone, M. G., Carbone, C., Faedo, D., Ferrero, L., Maggioni, A., Sangiorgi, G., and Bolzacchini, E.: Exhaust emissions of polycyclic aromatic hydrocarbons, n-alkanes and phenols from vehicles coming within different European classes, Atmos. Environ., 82, 391-400, https://doi.org/10.1016/j.atmosenv.2013.10.040, 2014.

Rogge, W. F., Hildemann, L. M., Mazurek, M. A., and Cass, G. R.: Sources of fine organic aerosol. 9. Pine, oak, and synthetic log combustion in residential fireplaces, Environ. Sci. technol., 32, 13-22, http://www.doi.org/10.1021/es960930b, 1998.

Ruehl, C. R., Nah, T., Isaacman, G., Worton, D. R., Chan, A. W. H., Kolesar, K. R., Cappa, C. D., Goldstein, A. H., and Wilson, K. R.: The influence of molecular structure and aerosol phase on the heterogeneous oxidation of normal and branched alkanes by OH, J. Phys. Chem. A., 117, 3990-4000, http://www.doi.org/10.1021/jp401888q, 2013.

Schauer, J. J., Kleeman, M. J., Cass, G. R., and Simoneit, B. R. T.: Measurement of emissions from air pollution sources. 1. C1 through C29 organic compounds from meat charbroiling, Environ. Sci. technol., 33, 1566-1577, http://www.doi.org/10.1021/es980076j, 1999.

Schauer, J. J., Kleeman, M. J., Cass, G. R., and Simoneit, B. R. T.: Measurement of emissions from air pollution sources. 3. C1−C29 organic compounds from fireplace combustion of wood, Environ. Sci. technol., 35, 1716-1728, http://www.doi.org/10.1021/es001331e, 2001.

Schauer, J. J., Kleeman, M. J., Cass, G. R., and Simoneit, B. R. T.: Measurement of emissions from air pollution sources. 4. C1−C27 organic compounds from cooking with seed oils, Environ. Sci. technol., 36, 567-575, http://www.doi.org/10.1021/es002053m, 2002a.

Schauer, J. J., Kleeman, M. J., Cass, G. R., and Simoneit, B. R. T.: Measurement of emissions from air pollution sources. 5. C1−C32 organic compounds from gasoline-powered motor vehicles, Environ. Sci. technol., 36, 1169-1180, http://www.doi.org/10.1021/es0108077, 2002b.

Schilling Fahnestock, K. A., Yee, L. D., Loza, C. L., Coggon, M. M., Schwantes, R., Zhang, X., Dalleska, N. F., and Seinfeld, J. H.: Secondary organic aerosol composition from C12 alkanes, J. Phys. Chem. A., 119, 4281-4297, http://www.doi.org/10.1021/jp501779w, 2015.

Yee, L. D., Craven, J. S., Loza, C. L., Schilling, K. A., Ng, N. L., Canagaratna, M. R., Ziemann, P. J., Flagan, R. C., and Seinfeld, J. H.: Secondary organic aerosol formation from low-NO_x photooxidation of dodecane: Evolution of multigeneration gas-phase chemistry and aerosol composition, J. Phys. Chem. A., 116, 6211-6230, http://www.doi.org/10.1021/jp211531h, 2012.

Zhang, H., Worton, D. R., Shen, S., Nah, T., Isaacman-VanWertz, G., Wilson, K. R., and Goldstein, A. H.: Fundamental time scales governing organic aerosol multiphase partitioning and oxidative aging, Environ. Sci. technol., 49, 9768-9777, http://www.doi.org/10.1021/acs.est.5b02115, 2015.

639 Zhao, Y., Hu, M., Slanina, S., and Zhang, Y.: The molecular distribution of fine particulate organic
640 matter emitted from Western-style fast food cooking, Atmos. Environ., 41, 8163-8171,
641 http://dx.doi.org/10.1016/j.atmosenv.2007.06.029, 2007a.
642
643 Zhao, Y., Hu, M., Slanina, S., and Zhang, Y.: Chemical compositions of fine particulate organic
644 matter emitted from Chinese cooking, Environ. Sci. Technol., 41, 99-105,
645 http://www.doi.org/10.1021/es0614518, 2007b.
646
647
648
649
650

651 **TABLE LEGENDS**
652
653 Table 1. The carbon preference index (CPI) and C_{max} for n-alkanals, n-alkan-2-ones, and
654 n-alkan-3-ones in this study and published data.
655
656 Table 2. Percentages of particle phase form and the partitioning coefficient Kp.
657
658 **FIGURE LEGENDS**
659
660 Figure 1. Map of the sampling sites. RU-Regents University (15 m above ground); WM-
661 University of Westminster (20 m above ground); EL-Eltham; MR-Marylebone Road
662 (south side).
663
664 Figure 2. The average total concentration of particle-bound n-alkanals (C_8-C_{20}), n-alkan-2-ones
665 (C_8-C_{26}), and n-alkan-3-ones (C_8-C_{19}), for each sampling period and site. The error bars
666 indicate one standard deviation.
667
668 Figure 3. Time series of particle-bound ∑1-alkanals, ∑n-alkan-2-ones and ∑n-alkan-3-ones at
669 RU, WM, EL, and MR sites.
670
671 Figure 4. The molecular distribution of particle-bound carbonyl compounds at four sites (RU,
672 WM, EL, and MR).
673
674
675

Atmospheric Chemistry and Physics Discussions

Atmos. Chem. Phys. Discuss., https://doi.org/10.5194/acp-2018-769
Manuscript under review for journal Atmos. Chem. Phys.
Discussion started: 3 September 2018

Table 1. The carbon preference index (CPI) and C_{max} for n-alkanals, n-alkan-2-ones, and n-alkan-3-ones in this study and published data.

Location / Sampling site	Sampling period	n-alkanals		n-alkan-2-ones		n-alkan-3-ones		Reference
		CPI	C_{max}	CPI	C_{max}	CPI	C_{max}	
RU, surrounded by Regent's Park, 15 m above ground	23 Jan - 19 Feb	0.52	C_8	1.23	C_{19}	1.30	C_{17}	Present study
WM, 20 m above ground	24 Jan - 20 Feb	0.41	C_8	0.99	C_{20}	1.26	C_{17}	Present study
EL, suburb of London	23 Feb - 21 Mar	0.71	C_8	1.57	C_{20}	1.04	C_{16}	Present study
MR, adjacent to Marylebone road	22 Mar - 18 Apr	1.07	C_8	0.57	C_{16}	1.12	C_{16}	Present study
Athens, Athinas St.	August	1.49	C_{15}, C_{17}	1.09	C_{18}, C_{21}, C_{19}			(Andreou and Rapsomanikis, 2009)
Urban roadside	March			3.26	C_{21}, C_{19}, C_{20}			
Athens, AEDA, Urban, 20 m above ground	March			2.41	C_{19}, C_{18}, C_{20}			(Andreou and Rapsomanikis, 2009)
Heraklion, Greece Urban 15 m above ground	Spring /summer	0.80–1.40	C_{26}, C_{28}	1.30–1.80	C_{23}, C_{29}, C_{31}			(Gogou et al., 1996)
Vancouver, Canada Roadway tunnel				1.33	C_{17}, C_{19}			(Cheng et al., 2006)
Aveiro, Portugal	Summer		C_{22}, C_{23}, C_{26}		C_{26}, C_{28}, C_{30}			
Suburban	Winter							(Oliveira et al., 2007)
K-Puszta, Hungary	Summer		C_{24}, C_{26}, C_{28}		C_{24}, C_{26}, C_{28}			

Atmos. Chem. Phys. Discuss., https://doi.org/10.5194/acp-2018-769
Manuscript under review for journal Atmos. Chem. Phys.
Discussion started: 3 September 2018

Atmospheric Chemistry and Physics Discussions

Table 2. Percentages of particle phase form and the partitioning coefficient Kp.

	RU						WM					
	n-alkanals		n-alkan-2-ones		n-alkan-3-ones		n-alkanals		n-alkan-2-ones		n-alkan-3-ones	
	%	Kp	%	Kp	%	Kp	%	Kp	%	Kp	%	Kp
C_8	82.9	1.16E-04	18.4	5.37E-06	23.9	7.47E-06	80.2	9.09E-05	13.3	3.43E-06	34.1	1.16E-05
C_9	69.2	5.37E-05	14.5	4.03E-06	16.6	4.74E-06	60.5	3.43E-05	15.6	4.16E-06	28.7	9.05E-06
C_{10}	75.3	7.27E-05	13.6	3.77E-06	7.43	1.92E-06	82.1	1.03E-04	14.4	3.77E-06	23.3	6.82E-06
C_{11}	45.5	1.99E-05	21.4	6.49E-06	12.8	3.49E-06	62.4	3.72E-05	20.1	5.65E-06	36.3	1.28E-05
C_{12}	74.8	7.08E-05	25.0	7.96E-06	31.3	1.09E-05	73.7	6.29E-05	28.8	9.07E-06	22.7	6.60E-06
C_{13}	82.9	1.15E-04	61.0	3.74E-05	35.4	1.31E-05	82.2	1.04E-04	48.9	2.14E-05	62.5	3.74E-05
C_{14}	82.8	1.15E-04	49.5	2.34E-05	35.5	1.31E-05	75.8	7.04E-05	31.8	1.05E-05	25.6	7.74E-06
C_{15}	99.5	5.01E-03	84.1	1.26E-04	50.5	2.44E-05	100		85.0	1.27E-04	68.5	4.87E-05
C_{16}	100		91.4	2.53E-04	70.3	5.64E-05	100		89.6	1.93E-04	91.7	2.47E-04
C_{17}	100		91.5	2.55E-04	100		100		85.9	1.36E-04	91.5	2.42E-04
C_{18}	100		94.1	3.80E-04	100		100		84.8	1.26E-04	99.4	4.02E-03
C_{19}	100		99.1	2.69E-03			100		100			
C_{20}	100		100				100		100			
C_{21}			100						100			
C_{22}			100						100			
C_{23}			100						100			
C_{24}			100						100			
C_{25}			100						100			
C_{26}			100						100			

Atmos. Chem. Phys. Discuss., https://doi.org/10.5194/acp-2018-769
Manuscript under review for journal Atmos. Chem. Phys.
Discussion started: 3 September 2018

Atmospheric Chemistry and Physics Discussions

	EI						MR					
	n-alkanals		n-alkan-2-ones		n-alkan-3-ones		n-alkanals		n-alkan-2-ones		n-alkan-3-ones	
	%	Kp	%	Kp	%	Kp	%	Kp	%	Kp	%	Kp
C_8	92.7	6.53E-04	24.9	1.72E-05	31.9	2.43E-05	90.0	2.94E-04	28.2	1.28E-05	43.0	2.46E-05
C_9	92.2	6.16E-04	38.0	3.18E-05	44.4	4.15E-05	89.9	2.89E-04	27.0	1.20E-05	39.1	2.09E-05
C_{10}	90.5	4.96E-04	47.6	4.70E-05	47.0	4.59E-05	91.7	3.62E-04	61.1	5.12E-05	20.4	8.33E-06
C_{11}	87.0	3.47E-04	72.3	1.35E-04	81.9	2.34E-04	87.4	2.26E-04	50.2	3.28E-05	33.1	1.61E-05
C_{12}	92.9	6.73E-04	83.4	2.60E-04	66.4	1.02E-04	93.0	4.30E-04	88.5	2.51E-04	28.1	1.28E-05
C_{13}	95.6	1.12E-03	82.2	2.40E-04	65.7	9.92E-05	96.1	8.04E-04	87.7	2.33E-04	46.2	2.79E-05
C_{14}	91.4	5.52E-04	90.3	4.80E-04	59.1	7.48E-05	95.2	6.51E-04	95.9	7.61E-04	72.0	8.38E-05
C_{15}	96.7	1.53E-03	94.5	8.98E-04	84.4	2.80E-04	100		96.9	1.02E-03	83.8	1.69E-04
C_{16}	100		96.7	1.41E-03	89.0	4.18E-04	100		96.4	8.70E-04	88.0	2.38E-04
C_{17}	100		95.1	1.00E-03	81.5	2.28E-04	100		96.0	7.73E-04	88.0	2.39E-04
C_{18}	100		64.6	9.44E-05	85.0	2.93E-04	100		92.5	4.04E-04	100	
C_{19}	100		100				100		100		100	
C_{20}	100		100				100		100			
C_{21}			100						100			
C_{22}			100						100			
C_{23}			100						100			
C_{24}									100			

Atmos. Chem. Phys. Discuss., https://doi.org/10.5194/acp-2018-769
Manuscript under review for journal Atmos. Chem. Phys.
Discussion started: 3 September 2018

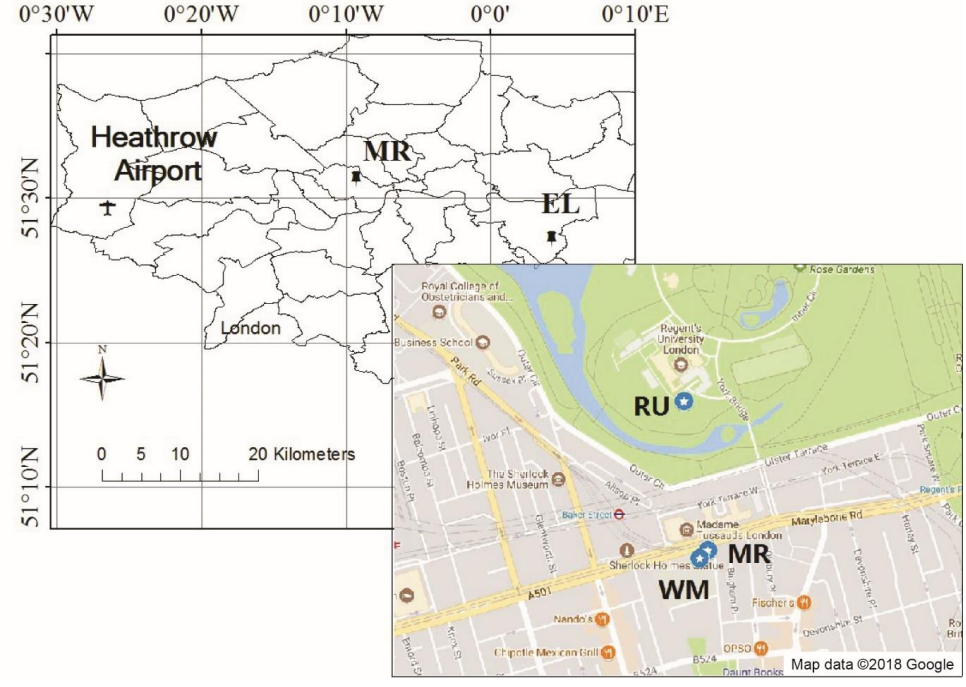

Fig. 1. Map of the sampling sites. RU-Regents University (15 m above ground); WM-University of Westminster (20 m above ground); EL-Eltham; MR-Marylebone Road (south side).

Atmos. Chem. Phys. Discuss., https://doi.org/10.5194/acp-2018-769
Manuscript under review for journal Atmos. Chem. Phys.
Discussion started: 3 September 2018

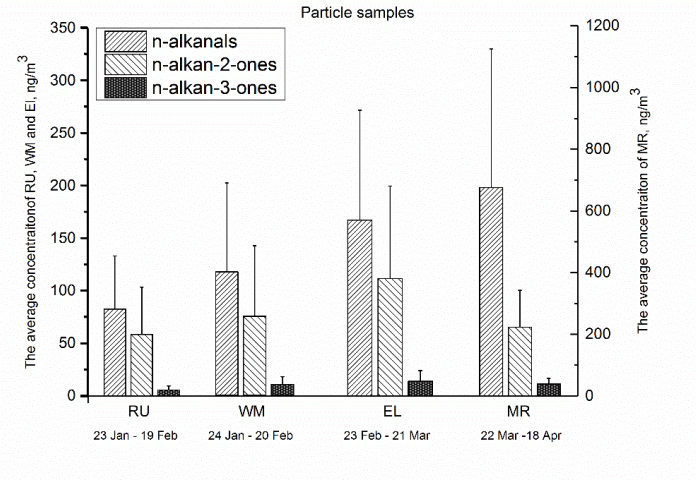

Fig. 2. The average total concentration of particle-bound n-alkanals (C_8-C_{20}), n-alkan-2-ones (C_8-C_{26}), and n-alkan-3-ones (C_8-C_{19}), for each sampling period and site. The error bars indicate one standard deviation.

Atmos. Chem. Phys. Discuss., https://doi.org/10.5194/acp-2018-769
Manuscript under review for journal Atmos. Chem. Phys.
Discussion started: 3 September 2018

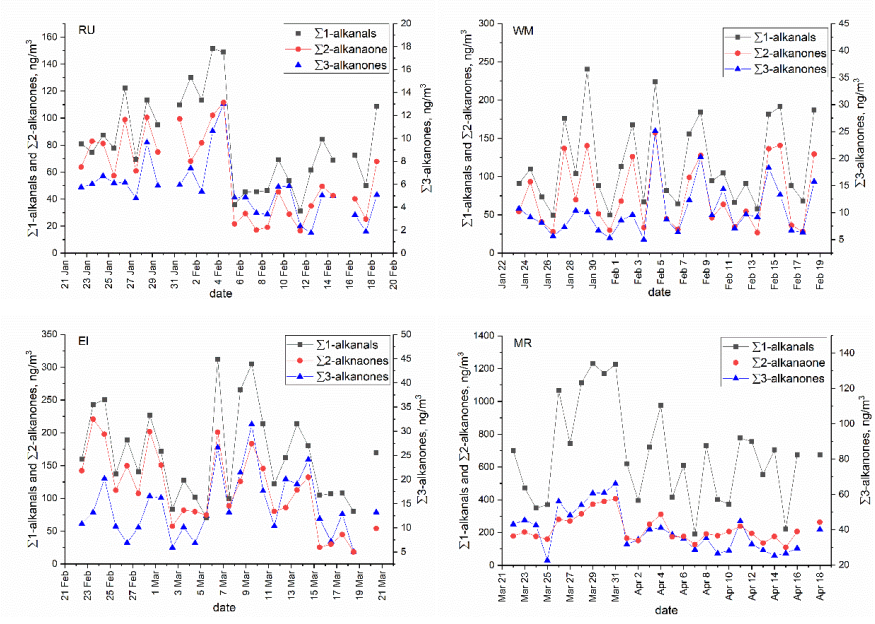

Fig. 3. Time series of particle-bound ∑1-alkanals, ∑n-alkan-2-ones and ∑n-alkan-3-ones at RU, WM, EL, and MR sites.

Atmos. Chem. Phys. Discuss., https://doi.org/10.5194/acp-2018-769
Manuscript under review for journal Atmos. Chem. Phys.
Discussion started: 3 September 2018

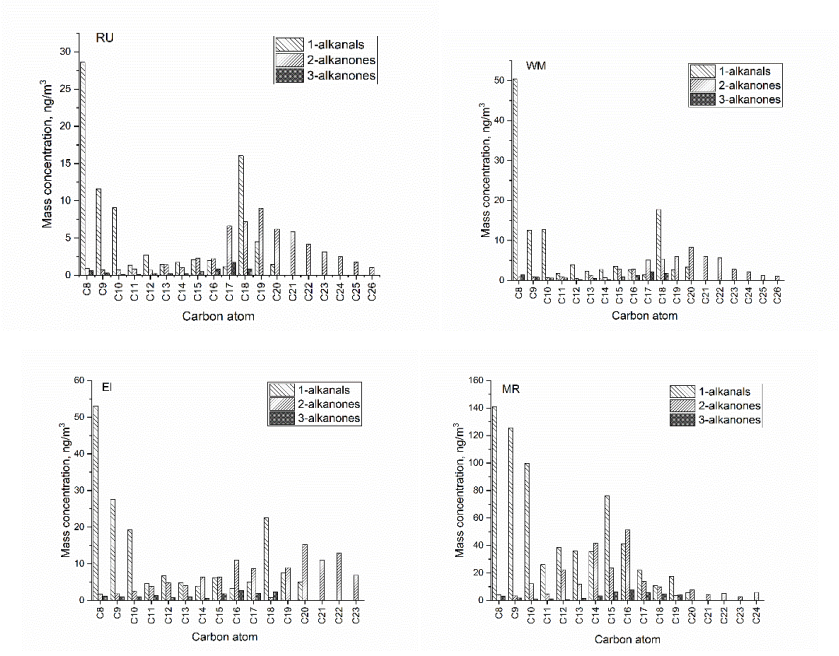

Fig. 4. The molecular distribution of particle-bound carbonyl compounds at four sites (RU, WM, EL, and MR).